

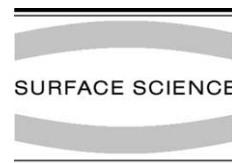


ELSEVIER

Available online at www.sciencedirect.com

SCIENCE @ DIRECT®

Surface Science 529 (2003) 151–157

www.elsevier.com/locate/susc

The surface of $\text{Sr}_2\text{Ru}_{0.9}\text{Mo}_{0.1}\text{O}_4$: a LEED and STM study

Ismail ^{a,b}, L. Petersen ^b, Jiandi Zhang ^{c,*}, R. Jin ^b, D.G. Mandrus ^{a,b},
E.W. Plummer ^{a,b}

^a Department of Physics and Astronomy, The University of Tennessee, Knoxville, TN 37996, USA

^b Solid State Division, Oak Ridge National Laboratory (ORNL), Oak Ridge, TN 37831, USA

^c Department of Physics, Florida International University, Miami, FL 33199, USA

Received 7 October 2002; accepted for publication 14 January 2003

Abstract

In the unconventional superconductor Sr_2RuO_4 , substitution of a small amount of Mo for Ru destroys the superconducting state. We have used low energy electron diffraction (LEED) and scanning tunneling microscopy (STM) to study the cleaved (100) surface of the Mo-doped strontium ruthenate: $\text{Sr}_2\text{Ru}_{0.9}\text{Mo}_{0.1}\text{O}_4$. Excellent LEED patterns indicate a well-ordered surface similar to Sr_2RuO_4 . The analysis of LEED- $I(V)$ spectra revealed that the (Ru/Mo) O_6 octahedra at the surface are rotated alternating clockwise and counterclockwise by $8.8^\circ \pm 2.5^\circ$ about the direction of the surface normal, which is identical to these on the surface of Sr_2RuO_4 . But the high-resolution STM images of $\text{Sr}_2\text{Ru}_{0.9}\text{Mo}_{0.1}\text{O}_4$ show a surface fundamentally different from that of Sr_2RuO_4 . The STM images are surprisingly inhomogeneous without clear atomic resolution. This indicates a local spatial roughness in the electronic structure induced by the Mo doping.

© 2003 Elsevier Science B.V. All rights reserved.

Keywords: Low energy electron diffraction (LEED); Scanning tunneling microscopy; Surface relaxation and reconstruction

The discovery of unconventional superconductivity in Sr_2RuO_4 (with the intrinsic transition temperature $T_C \sim 1.5$ K) has evoked strong interests because it is the first layered-perovskite superconductor without doping [1,2]. The possible spin-triplet pairing mechanism [3] for the superconducting phase has promoted deeper investigation of its anisotropic and unconventional physical properties in both superconducting and normal states. One of the least ambiguous properties of its unconventional superconductivity is a pronounced

sensitivity to nonmagnetic impurities/defects [4,5]. By replacing a tiny portion (5%) of the Sr^{2+} by Ca^{2+} in Sr_2RuO_4 , the superconducting state disappears even though the lattice structure is almost unchanged [6,7]. Similar behavior occurs when using Mo^{4+} to replace a tiny fraction of Ru^{4+} in Sr_2RuO_4 [8]. Thus, the strong suppression of superconductivity by impurity may be related to the strong impurity influence [9] on the magnetic fluctuations, which are believed to play a key role for the unusual properties in Sr_2RuO_4 [3]. Ferromagnetic (FM) spin fluctuations that are associated mostly with the 2D-like d_{xy} orbital were proposed to mediate the spin-triplet pairing mechanism for the superconductivity [3]. ^{17}O NMR

* Corresponding author.

E-mail address: zhangj@fiu.edu (J. Zhang).

measurements from Sr_2RuO_4 indeed revealed such orbital-dependent FM correlations at $\mathbf{q} = \mathbf{0}$ [10]. On the other hand, band structure calculations predicted antiferromagnetic (AFM) spin fluctuations at incommensurate positions arising from the Fermi-surface nesting in the 1D-like bands associated with the d_{xz} and d_{yz} t_{2g} -Ru orbitals [11]. Inelastic neutron scattering has confirmed this nesting scenario [12] with a strong magnetic susceptibility feature located at an incommensurate wave number $\mathbf{q} \cong (2\pi/3a, 2\pi/3a, 0)$. These suggest a possibility of the competition between FM and AFM spin fluctuations, leading to a competition between spin triplet and spin singlet superconductivity in Sr_2RuO_4 [11]. Thus the roles of these band-specific spin fluctuations in the pairing symmetry and mechanism are a subject of active investigations [13] and the effect of impurity on spin fluctuations is surely a central issue [14].

In many cases, a tiny amount of doping or chemical substitution to certain transition-metal oxides (TMOs) can act as an impurity that could change *local* or even global physical properties significantly [15]. Therefore, it is imperative to study the local impurity effect on both the electronic and structural properties by doping or chemical substitution, which can be pursued for example by using scanning tunneling microscopy (STM). In this letter, we report a study of the surface of $\text{Sr}_2\text{Ru}_{0.9}\text{Mo}_{0.1}\text{O}_4$ using both low energy electron diffraction (LEED) and STM, to investigate the effect of the chemical substitution on the surface structural and *local* electronic properties. While Sr_2MoO_4 has the same crystal structure as Sr_2RuO_4 with 1% larger lattice constants a and c , no sign of superconductivity is observed [16], suggesting distinct ground states between these two materials.

We find with LEED I - V analysis that the cleavable (001) surface of $\text{Sr}_2\text{Ru}_{0.9}\text{Mo}_{0.1}\text{O}_4$ displays long-range order and reconstruction into a lattice structure with a $p4gm$ symmetry. Similar to what was obtained from undoped Sr_2RuO_4 [17–19], the (Ru/Mo) O_6 octahedra at the surface of $\text{Sr}_2\text{Ru}_{0.9}\text{Mo}_{0.1}\text{O}_4$ are rotated about the c -axis by $8.5 \pm 2.5^\circ$ from the ideal K_2NF_4 -type bulk structure. However, such reconstruction cannot be

clearly revealed by STM images due to electronic inhomogeneity. We argue that there are strong nonlinear impurity effects on surface electronic structure of $\text{Sr}_2\text{Ru}_{0.9}\text{Mo}_{0.1}\text{O}_4$.

Single crystals of $\text{Sr}_2\text{Ru}_{0.9}\text{Mo}_{0.1}\text{O}_4$ were grown by the floating zone technique with an NEC SC-M15HD image furnace. For feed-rod preparation, a mixture of SrCO_3 , RuO_2 , and MoO_2 , with molar ratio of 2.0:1.0:0.1, was pre-reacted in air at 1100 °C for 10 h. After regrinding, the powder was pressed into rods and heated in air at 850 °C for another 10 h. Single crystals were grown using a feed rate of 30 mm/h and a growth rate of 15 mm/h in an atmosphere of 10% oxygen and 90% argon under pressure of 0.2 MPa. Shiny black crystals are produced with actual Ru:Mo \sim 0.92:0.08 as determined by energy dispersive X-ray analysis. The sample was glued to a sample holder with silver-epoxy and a metal-post was glued on top of the sample. After being introduced to the vacuum chamber, the sample was cleaved either at 90 K or at room temperature and the (100) surface was obtained.

The experiments were performed under ultra-high vacuum conditions in a chamber with a base pressure of $\sim 1.0 \times 10^{-10}$ Torr. The chamber is equipped with an Omicron LEED- $I(V)$ setup and an Omicron Variable temperature STM. Intensities of the LEED beams as a function of incident electron energy (i.e., LEED- $I(V)$ spectra) were measured with the sample temperature held at 90 K. We observed no obvious changes in surface structure with varying temperature from 90 K to room temperature. The normal incidence of incident electron beam was achieved by adjusting the position of the sample until I - V curves of symmetrically equivalent beams were identical. All available equivalent beams were averaged and normalized by incident electron beam current. Finally, we had five nonequivalent integer beams (1,0), (2,0), (2,1), (2,2), (3,0) in a total energy range of 2220 eV and three nonequivalent fractional beams (1.5,0.5), (2.5,0.5), and (2.5,1.5) with a total energy range of 420 eV. The STM imaging was also performed at 90 K and at room temperature. Before we performed STM experiments on $\text{Sr}_2\text{Ru}_{0.9}\text{Mo}_{0.1}\text{O}_4$, the STM tip was calibrated by scanning on a cleaned Ge(1 1 1) surface where nice

images with excellent atomic resolution were routinely obtained.

Analysis of the LEED- $I(V)$ spectra was carried out using standard multiple scattering algorithms combined with automated tensor-LEED programs of Barbieri and Van Hove [20]. Thirteen atomic phase shifts for Sr, Ru, Mo, and O were derived from the muffin-tin potential approximation and employed in our calculations. The average t -matrix approximation was applied in the calculations, as has been used for the structural determination of random alloys [21]. The ratio of the chemical concentration between Ru and Mo in the surface layer was relaxed in our calculations and was found to be the same as in the bulk with no sign of surface segregation. A full dynamical calculation for the initial reference structure was performed by using the Beeby matrix inversion scheme where multiple scattering within a layer was treated exactly and renormalized forward scattering for stacking layers was employed [22]. Electron attenuation was described by an optical potential; the real part (V_{or}) was constant and optimized during the search, while the imaginary part (V_{oi}) was modeled by $V_{oi} = V_i \{E / (200 / 27.21 + V_{or})\}^{1/3}$ where E is the incident electron energy (eV) and V_i and V_{or} are constants optimized during the search. The temperature effect was included through the multiplication of atomic scattering matrix with a Debye Waller factor, where the Debye temperature optimized in the calculations was converted into isotropic mean-square displacements. The tensor-LEED approximation method was used for the structural determination [23]. Calculated intensities ($I-V$) were compared to the experimental data by using the Pendry's R -factor (R_p) [20], and the error-bar calculated as defined by Pendry [24]. The lattice constants used in the calculation are $a = 3.87 \text{ \AA}$ and $c = 12.74 \text{ \AA}$ [25].

Fig. 1(a) shows a typical LEED pattern from the cleaved surface of $\text{Sr}_2\text{Ru}_{0.9}\text{Mo}_{0.1}\text{O}_4$ at 90 K obtained with electron energy of 200 eV, showing excellent diffraction spots from both integer and fractional beams, similar to the situation for the un-doped Sr_2RuO_4 [17,18]. As shown in Fig. 2, a comparison of the line profile of the intensity of both integer and fractional LEED spots from both surfaces clearly indicates the identical quality of

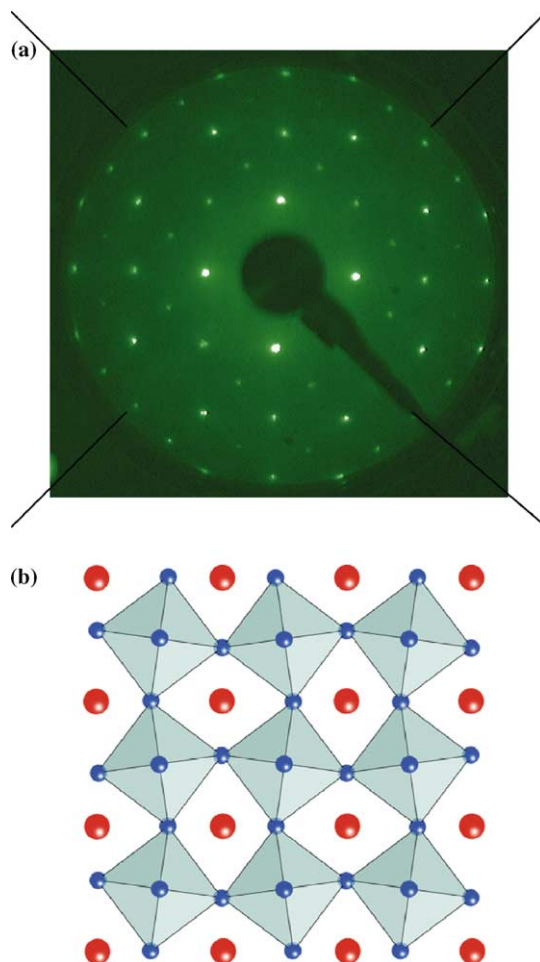


Fig. 1. (a) A typical LEED pattern from vacuum cleaved (100) surface of single crystal $\text{Sr}_2\text{Ru}_{0.9}\text{Mo}_{0.1}\text{O}_4$, taken at sample temperature $T = 90 \text{ K}$ with an electron beam energy of 200 eV. The fractional spots are clearly seen indicating a surface $(\sqrt{2} \times \sqrt{2})R45^\circ$ reconstruction. (b) Top view of the reconstructed surface structure of $\text{Sr}_2\text{Ru}_{0.9}\text{Mo}_{0.1}\text{O}_4$, which is identical to that of Sr_2RuO_4 [19]. The big balls represent strontium atoms, small balls oxygen.

the surface lattice ordering. Furthermore, the diffraction pattern from this surface is identical to that obtained from the un-doped Sr_2RuO_4 [17,18], indicating a clear surface reconstruction. Some fractional beams such as (0.5,0.5), (1.5,1.5) and (2.5,2.5) are extinct at all incident electron energies, confirming that the surface reconstruction has the glide-line symmetry with two perpendicular-glide lines along the direction of the missing

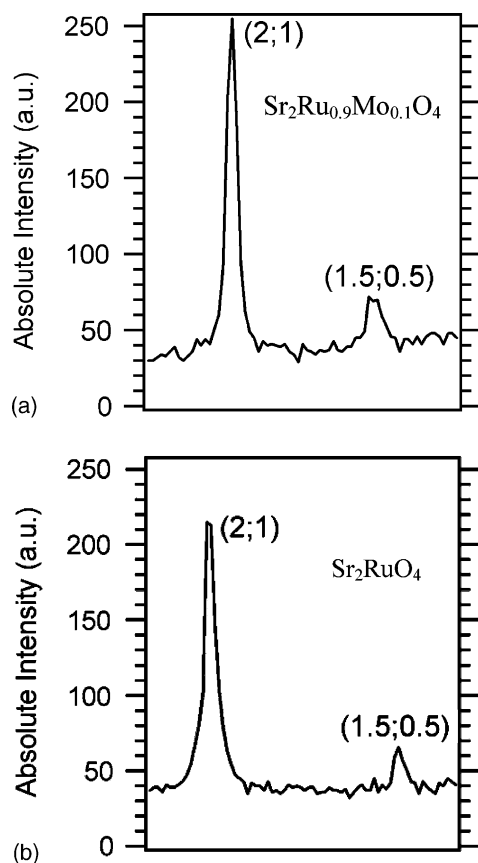


Fig. 2. The line profile of the intensity of both integer and fractional LEED spots from the surfaces of $\text{Sr}_2\text{Ru}_{0.9}\text{Mo}_{0.1}\text{O}_4$ (top) and Sr_2RuO_4 (bottom), taken at $T = 90$ K with an electron beam energy of 190 eV. The identical intensity ratios of LEED spots to background taken from both surfaces indicate identical surface ordering in lattice structure.

spots. This behavior is exactly the same as that observed in Sr_2RuO_4 , where the surface structure has $p4gm$ symmetry [18]. We have refined the lattice structure by restricting the symmetry to $p4gm$.

The optimized Debye temperatures are 600 K for Sr, 660 K for Ru, 250 K for Mo, and 1480 K for O, respectively. The agreement between calculated and experimental LEED- $I(V)$ spectra is excellent, reflected by the total Rp -factor of 0.15 for the total energy range of 2640 eV. For comparison, with Sr_2RuO_4 the total Rp -factor was 0.17 for the total energy range of 2045 eV [18]. We found that the surface structure is distorted from the bulk, as the $(\text{Ru}/\text{Mo})\text{O}_6$ octahedra at the surface are rotated by $8.8^\circ \pm 2.5^\circ$ clockwise and counterclockwise about the c -axis perpendicular to the surface, as schematically shown in Fig. 1(b). The vertical displacements of the atoms at the surface do not deviate significantly from the corresponding bulk positions (see Table 1). At the surface, the bond length of $\text{Ru}/\text{Mo}-\text{O}(2)$ (perpendicular to the surface) is found to be 2.038 ± 0.03 Å, and the bond length of $\text{Ru}/\text{Mo}-\text{O}(1)$ (parallel to the surface) is 1.954 ± 0.03 Å. These values are about the same as for Sr_2RuO_4 , 2.065 Å (perpendicular to the surface) and 1.952 Å (parallel to the surface) [18]. There was no out-of-plane (i.e., along c -axis) tilt distortion of the octahedra observed.

Lattice distortions in TMOs are commonly due to stress in the lattice depending on the ionic radius ratios. For example, the bulk structure of Sr_2RuO_4 is not distorted, i.e., the octahedra are not rotated or tilted from ideal rock-salt type structure. But Ca_2RuO_4 is strongly distorted by tilt and rotation of the octahedra due to the small radius of the calcium ion as compared to the strontium ion [26]. The replacement of the transition metal ion by other ions with different ionic radius also results in lattice distortions. For example, the substitution of Ir or Rh for Ru in Sr_2RuO_4 results in a rigid rotation of the octahedra in bulk about the c -axis by 11° for Sr_2IrO_4 , [27]

Table 1

Vertical displacements of the atoms in the surface layer with respect to the bulk structure as determined by the structure refinement from LEED- $I(V)$ spectra

| Vertical displacement (Å) | First layer | Second layer | Third layer |
|---------------------------|--------------------|--------------------|--------------------|
| O | -0.008 ± 0.030 | -0.013 ± 0.040 | -0.030 ± 0.050 |
| Sr | -0.040 ± 0.015 | – | $+0.016 \pm 0.025$ |
| Ru/Mo | – | -0.034 ± 0.030 | – |

Negative (positive) sign indicates the atom moves upward (downward).

and by 10° for Sr_2RhO_4 [28]. In Sr_2RuO_4 , the surface lattice distortion is actually a frozen phonon structure, corresponding to the Σ_3 bulk-phonon mode that is softened near the zone boundary in the bulk [29]. As noted above, both surfaces of the un-doped (Sr_2RuO_4) and doped ($\text{Sr}_2\text{Ru}_{0.9}\text{Mo}_{0.1}\text{O}_4$) ruthenates exhibit an identical in-plane rotational distortion of the octahedra. Thus we expect the same mechanism for the lattice distortion at both surfaces. The frozen-phonon surface reconstruction is the result of broken symmetry by creating the surface.

Based upon the similar lattice structure determined from LEED results, one would expect that an STM study on $\text{Sr}_2\text{Ru}_{0.9}\text{Mo}_{0.1}\text{O}_4$ should reveal similar surface topography as Sr_2RuO_4 , where the reconstruction was revealed clearly from atomically resolved images. However, the STM images on the surface of $\text{Sr}_2\text{Ru}_{0.9}\text{Mo}_{0.1}\text{O}_4$ present completely unexpected results. Fig. 3 shows a large-scale STM image of $\text{Sr}_2\text{Ru}_{0.9}\text{Mo}_{0.1}\text{O}_4$, revealing large flat terraces with clear steps similar to these observed from Sr_2RuO_4 . Line scans show that the step height is about 6 \AA , corresponding to half the height of the unit cell in the (001) direction ($c = 12.74 \text{ \AA}$ [19]), where c -axis is normal to the surface. This observation is consistent with that the top surface layer is the SrO plane as determined from our LEED results. However, the high-resolution STM image of $\text{Sr}_2\text{Ru}_{0.9}\text{Mo}_{0.1}\text{O}_4$ is surprisingly different from that of Sr_2RuO_4 . To avoid “tunnel version”, we sampled many different areas with the STM, and obtained similar results. Fig. 4 shows a representative high-resolution STM image as well as a line profile taken from the STM image of $\text{Sr}_2\text{Ru}_{0.9}\text{Mo}_{0.1}\text{O}_4$. In contrast to what obtained in Sr_2RuO_4 [17–19] the atomic resolution is poor in $\text{Sr}_2\text{Ru}_{0.9}\text{Mo}_{0.1}\text{O}_4$. The surface appears rather disordered, with a surface roughness of about 0.6 \AA , which is significantly larger than the atomic corrugation observed for Sr_2RuO_4 (0.25 \AA). The main structural element seems to be “blobs” that are roughly 5 \AA in size (see the line profile in Fig. 4(b)). In view of Fig. 4(a), these blobs seem somewhat ordered locally. However a Fourier transform of the image only shows very weak spots that could potentially be associated with lattice order. By imaging the surfaces cleaved

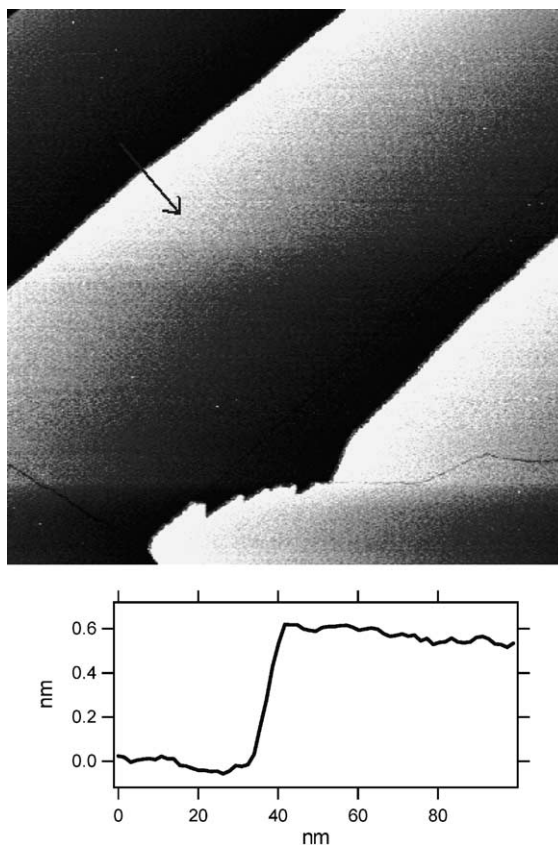


Fig. 3. Large-scale STM image ($600 \times 600 \text{ nm}^2$) of $\text{Sr}_2\text{Ru}_{0.9}\text{Mo}_{0.1}\text{O}_4$ cleaved in vacuum (top) with a line scan indicated (the arrow). Bottom figure is the line scan showing a step height of about 6 \AA .

at both 90 K and room temperature, no obvious difference has been observed.

Apparently, the disordered nature of STM data is inconsistent with the beautifully ordered LEED images. The sharp LEED patterns without diffuse background indicate a long-range lattice ordering with a coherent length of $\sim 200 \text{ \AA}$. While the STM image, at best can be interpreted as a disordered array of small semi-ordered regions, with a size of less than 50 \AA . To reconcile the similarity of the LEED patterns but the dissimilarity of the STM images in Sr_2RuO_4 and $\text{Sr}_2\text{Ru}_{0.9}\text{Mo}_{0.1}\text{O}_4$, one should focus on the physical principles governing the two techniques. LEED depends on scattering from an ion core, and is insensitive to the valence electrons. In contrast, STM images are almost

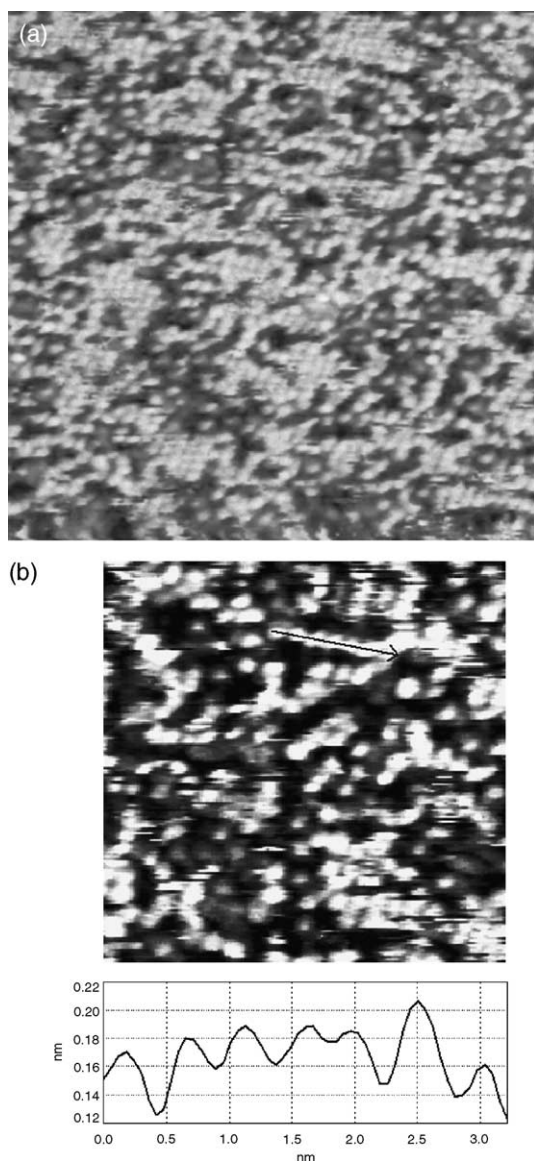


Fig. 4. High-resolution STM images ($25 \times 25 \text{ nm}^2$ in (a) and $10 \times 10 \text{ nm}^2$ in (b)) of $\text{Sr}_2\text{Ru}_{0.9}\text{Mo}_{0.1}\text{O}_4$ taken at room temperature with sample bias voltage $+0.86 \text{ V}$ and current 0.2 nA . A line profile of image is also shown in (b) indicating the size ($\sim 5 \text{ \AA}$) of these main structural “blobs”.

solely influenced by the valence electrons as they can be interpreted as a fingerprint of the local density of states at the surface layer. Thus, the surface disorder/roughness of $\text{Sr}_2\text{Ru}_{0.9}\text{Mo}_{0.1}\text{O}_4$ revealed by STM must be related to electronic

inhomogeneities, and not to structural disorder. A very recent study reports that homogeneous doping is *not* always the case [30], and there is evidence of chemical and structural inhomogeneity in lightly doped $\text{La}_{1-x}\text{Sr}_x\text{MnO}_3$ for $x < 0.3$. If the Mo doping indeed induces spatial electronic inhomogeneity even though there are no obvious changes in lattice structure, then this may correlate with the extremely strong suppression of the superconductivity in Sr_2RuO_4 caused by defects or doped impurities [4–8]. These impurities/defects may act as pair breakers that can severely suppress the superconducting transition temperature (T_C), though further understanding for the role of these impurities on the electronic structure is necessary.

In summary, we have studied the surface of a Mo-doped strontium ruthenate. We have found that both surfaces with and without Mo-doped Sr_2RuO_4 exhibit an identical structural reconstruction, presumably due to the similar frozen-phonon structure at the surface. Surprisingly, the STM images reveal that the surface of $\text{Sr}_2\text{Ru}_{0.9}\text{Mo}_{0.1}\text{O}_4$ is electronically rough and disordered, in sharp contrast to the surface of Sr_2RuO_4 . These may indicate that the Mo dopants drastically affect the *local* electronic structure, causing the strong suppression of the superconducting state existing in Sr_2RuO_4 .

Acknowledgements

We acknowledge the use of the Barbieri/Van Hove Symmetrized Automated Tensor LEED package, available from M.A. Van Hove. One of us (L.P.) gratefully acknowledges a Eugene P. Wigner fellowship at Oak Ridge National Laboratory. This work was funded by National Science Foundation grant DMR-0072998, and the US Department of Energy under contract DE-AC05-00OR22725 with the Oak Ridge National Laboratory, managed by UT-Battelle, LLC.

References

- [1] Y. Maeno, H. Hashimoto, K. Yoshida, S. Nashizaki, T. Fujita, J.G. Bednorz, F. Lichtenberg, *Nature (London)* 372 (1994) 532.

- [2] Y. Maeno, T.M. Rice, M. Sigrist, *Phys. Today* 54 (2001) 42.
- [3] T.M. Rice, M. Sigrist, *J. Phys.: Condens. Matter* 7 (1995) L643.
- [4] A.P. Mackenzie, R.K.W. Haselwimmer, A.W. Tyler, G.G. Lonzarich, Y. Mori, S. Nishizaki, Y. Maeno, *Phys. Rev. Lett.* 80 (1998) 161.
- [5] Z.Q. Mao, Y. Mori, Y. Maeno, *Phys. Rev. B* 60 (1999) 610.
- [6] O. Friedt, M. Braden, G. Andre, P. Adelman, S. Nakatsudji, Y. Maeno, *Phys. Rev. B* 63 (2001) 174432.
- [7] S. Nakatsuji, Y. Maeno, *Phys. Rev. Lett.* 84 (2000) 2666.
- [8] S.-I. Ikeda, N. Shirakawa, H. Bando, Y. Ootuka, *J. Phys. Soc. Jpn.* 69 (2000) 3162.
- [9] M. Minakata, Y. Maeno, *Phys. Rev. B* 63 (2001) 180504; M. Braden, O. Friedt, Y. Sidis, P. Bourges, M. Minakata, Y. Maeno, *Phys. Rev. Lett.* 88 (2002) 197002.
- [10] T. Imai, A.W. Hunt, K.R. Thurber, F.C. Chou, *Phys. Rev. Lett.* 81 (1998) 3006.
- [11] I.I. Mazin, D.J. Singh, *Phys. Rev. Lett.* 79 (1997) 733, *Phys. Rev. Lett.* 82 (1999) 4234.
- [12] Y. Sidis, M. Braden, P. Bourges, B. Hennion, S. NishiZaki, Y. Maeno, Y. Mori, *Phys. Rev. Lett.* 83 (1999) 3320.
- [13] K. Miyake, O. Narikiyo, *Phys. Rev. Lett.* 83 (1999) 1423; T. Kuwabara, M. Ogata, *Phys. Rev. Lett.* 85 (2000) 4586; M. Sato, M. Lohmoto, *J. Phys. Soc. Jpn.* 69 (2000) 3505.
- [14] D.K. Morr, P.F. Trautman, M.J. Graf, *Phys. Rev. Lett.* 86 (2001) 5978; N. Kikugawa, Y. Maeno, *Phys. Rev. Lett.* 89 (2002) 117001.
- [15] M. Imada, A. Fujimori, Y. Tokura, *Rev. Mod. Phys.* 70 (1998) 1039.
- [16] N. Shirakawa, S.I. Ikeda, *Physica C* 341 (2000) 783.
- [17] R. Matzdorf, Z. Fang, Ismail, J. Zhang, T. Kimura, Y. Tokura, K. Terakura, E.W. Plummer, *Science* 289 (2000) 746.
- [18] R. Matzdorf, Ismail, T. Kimura, Y. Tokura, E.W. Plummer, *Phys. Rev. B* 65 (2002) 85404.
- [19] E.W. Plummer, Ismail, R. Matzforf, A.V. Melecko, J. Zhang, *Prog. Surf. Sci.* 67 (2001) 17.
- [20] A. Barbieri, M.A. Van Hove, private communication.
- [21] S. Crampin, P.J. Rous, *Surf. Sci. Lett.* 244 (1991) L137.
- [22] J.B. Pendry, *Low Energy Electron Diffraction*, Academic Press, London, 1974.
- [23] P.J. Rous et al., *Phys. Rev. Lett.* 57 (1986) 2951; P.J. Rous, J.B. Pendry, *Surf. Sci.* 219 (1989) 355; P.J. Rous, M.A. Van Hove, G.A. Somorjai, *Surf. Sci.* 226 (1990) 15.
- [24] J.B. Pendry, *J. Phys. C* 13 (1980) 937.
- [25] O. Chmaissem, J.D. Jorgensen, H. Shaked, S. Ikeda, Y. Maeno, *Phys. Rev. B* 57 (1998) 5067.
- [26] M.A. Subramanian et al., *Physica C* 235 (1994) 743.
- [27] M.K. Crawford et al., *Phys. Rev. B* 49 (1994) 9198.
- [28] S.I. Ikeda, N. Shirakawa, H. Bando, Y. Ootuka, *J. Phys. Soc. Jpn.* 69 (2000) 3162.
- [29] M. Braden, W. Reidhardt, Y. Mori, S. Nishizaki, Y. Maeno, *Phys. Rev. B* 57 (1998) 1236.
- [30] T. Shibata, B. Bunker, J. Mitchell, P. Schiffer, *Phys. Rev. Lett.* 88 (2002) 207205.